JOURNAL OF SOLID STATE CHEMISTRY **127,** 131–135 (1996)
ARTICLE NO. 0368

LETTER TO THE EDITOR

Low Temperature Orthorhombic to Monoclinic Transition Due to Size Effect in $Nd_{0.7}Ca_{0.3-x}Sr_xMnO_3$: Evidence for a New Type of Charge Ordering

F. Millange, V. Caignaert, G. Mather, E. Suard,* and B. Raveau

*Laboratoire CRISMAT, URA 1318 associé au CNRS, ISMRA et Université de Caen 6, Boulevard du Maréchal Juin, 14050 Caen Cedex, France; and *Institut Laue-Langevin, 156X, Centre de tri, 38042 Grenoble Cedex, France*

Communicated by J. Mottorig, October 1, 1996

The structures of the perovskites $Nd_{0.7}Ca_{0.30-x}Sr_xMnO_3$ have been determined at 293 and 1.7 K for $x = 0$, 0.08, and 0.3. All these manganites, except the low-temperature form of $Nd_{0.7}Ca_{0.3}MnO_3$ ($x = 0$), exhibit the classical orthorhombic *Pnma* ($GdFeO_3$) structure. For $Nd_{0.7}Ca_{0.3}MnO_3$, a monoclinic structure, involving a new kind of charge ordering, is observed at 1.7 K. The importance of this phenomenon for the understanding of the CMR properties of these materials is emphasized.

Manganese perovskites have been the subject of considerable investigation since the discovery of their colossal magnetoresistance (CMR) properties (1–3). Extremely high resistance ratios of several orders of magnitude have been observed recently by applying a magnetic field of several tesla, as shown for instance for the praseodymium manganites (4). In all the perovskite manganites which exhibit CMR properties, manganese is present in both of the Mn^{3+} and Mn^{4+} valence states. For the $Ln_{0.5}Sr_{0.5}MnO_3$ manganites, a 1:1 charge ordering of the Mn^{3+} and Mn^{4+} ions takes place at low temperature (5–8). Many other types of order of the Mn^{3+} and Mn^{4+} species should be made possible by varying the Mn^{3+}/Mn^{4+} ratio (x) in the series $Ln_{1-x}A_xMnO_3$; to date, however, the 1:1 order is the only type that has been observed in these systems. It is probable that ordering will be greatly influenced by the average size of the interpolated cation, since the latter influences the Mn–O–Mn angle and the Mn–Mn distance and consequently the bandwidth, as shown from the results recently obtained for the manganites $Ln_{0.7}Ca_{0.3-x}Sr_xMnO_3$ (9, 10).

In our recent studies of the CMR manganites $Nd_{0.7}Ca_{0.3-x}Sr_xMnO_3$ (11), a progressive evolution from an insulating to a metallic state in a zero magnetic field at low temperature was observed by increasing x from 0 to 0.3 (Fig. 1). The CMR effect is exhibited on the application of a magnetic field. For example, material of composition $x = 0.08$ shows a resistance ratio ($R_o/R_{H=5\,T}$) of 10^6 at 50 K. An important factor for understanding the CMR properties of these materials concerns the crystallographic nature of the phase in the low-temperature domain, and especially the possibility of charge ordering at low temperature. For this reason, we have studied the crystal structure of these compounds versus temperature by powder neutron diffraction and high resolution electron microscopy. The complete results of this exhaustive study will be published elsewhere. Here, we present the neutron diffraction study results on three compositions ($x = 0$, 0.08, and 0.30) at 1.7 and 293 K: our study indicates that $x = 0$ has a monoclinic perovskite structure at low temperature, characterized by a new type of charge ordering.

The compounds were prepared by standard solid state reaction in air (11). Neutron powder data were collected on the high resolution powder diffractometer D2B (ILL Grenoble) using a wavelength $\lambda = 1.5938$ Å. An additional diffraction pattern was collected in a high resolution configuration with a wavelength of 2.39 Å, using a pyrolitic graphite filter in the primary beam. Data in the range $15° \leq 2\theta \leq 160°$ were refined by the Rietveld method using the program FULLPROF.

At room temperature, all three compounds exhibit the orthorhombic $GdFeO_3$ structure ($a \approx a_p\sqrt{2}$, $b \approx 2a_p$, $c \approx a_p\sqrt{2}$); the b and c parameters decrease as x decreases, whereas the a parameter increases (Table 1). This orthorhombic phase is isotypic with that described previously for $Pr_{0.7}Ca_{0.3-x}Sr_xMnO_3$ (12), so that its structure can be described in the same space group *Pnma*. The refined atomic coordinates are listed in Table 1. The corresponding interatomic distances and bond angles (Table 1) show two

0022-4596/96 $18.00

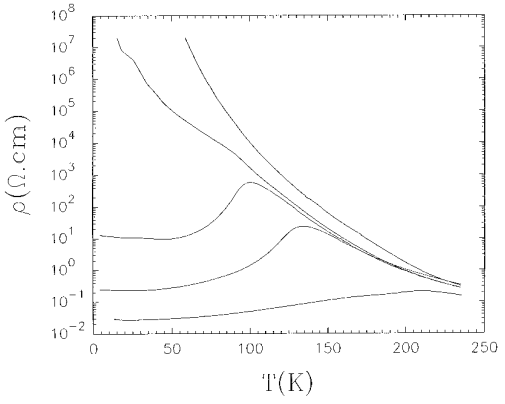

FIG. 1. T dependence of the resistivity at $B = 0$ for $Nd_{0.7}Ca_{0.3-x}Sr_xMnO_3$ (from top to bottom $x = 0$, 0.08, 0.10, 0.15, and 0.3).

interesting features: (i) the Jahn–Teller distortion of the MnO_6 octahedra increases significantly as x decreases, i.e., as the average size of the A-site cation decreases, ranging from 1.955–1.968 Å for $x = 0.30$, to 1.953–1.983 Å for $x = 0.08$, and to 1.953–1.992 Å for $x = 0$. (ii) The Mn–O–Mn bond angles deviate significantly from 180° with decreasing x, ranging from 158°70–159°90 for $x = 0.30$ to 155°41–154°90 for $x = 0$.

At low temperature, down to 1.7 K, the powder neutron diffraction patterns of the phases corresponding to $x = 0.30$ and $x = 0.08$ are still characteristic of the orthorhombic structure. The cell parameters and atomic coordinates are close to those observed at room temperature, and consequently the interatomic distances and bond angles do not vary significantly. By contrast, the neutron diffraction pattern of $Nd_{0.7}Ca_{0.3}MnO_3$ ($x = 0$) registered at 1.7 K (Fig. 2) shows a significant splitting of several peaks (inset of Fig. 2) and can only be indexed on a monoclinic unit cell with $a = 5.488\text{Å} \approx a_p\sqrt{2}$, $b = 7.634$ Å $\approx 2a_p$, $c = 5.397\text{Å} \approx a_p\sqrt{2}$, and $\beta = 90.20°$. Consequently, the structure of this phase was refined successfully in the space group $P2_1/m$, with Nd and Mn magnetic moments aligned along the b axis of the unit cell, yielding the following R factors: $R_p = 4.67\%$, $R_{wp} = 5.80\%$, and $\chi^2 = 1.80$. The atomic coordinates, interatomic distances, and bond angles of this phase, listed in Table 2, show the existence of two different sites for manganese. The Mn(1) site exhibits an average Mn–O distance of 1.95 Å and can be considered as randomly occupied by both Mn^{4+} (60%) and Mn^{3+} ions

TABLE 1
Room Temperature Structures

Space group: *Pnma*								
$Nd_{0.7}Sr_{0.3}MnO_3$				$Nd_{0.7}Sr_{0.08}Ca_{0.22}MnO_3$				$Nd_{0.7}Ca_{0.3}MnO_3$			
Cell parameters				Cell parameters				Cell parameters			
$a = 5.4599(1)$ Å				$a = 5.4708(1)$ Å				$a = 5.4820(1)$ Å			
$b = 7.7110(1)$ Å				$b = 7.6708(1)$ Å				$b = 7.6475(1)$ Å			
$c = 5.4660(1)$ Å				$c = 5.4254(1)$ Å				$c = 5.4096(1)$ Å			
Atomic coordinates				Atomic coordinates				Atomic coordinates			
	x	y	z		x	y	z		x	y	z
A	0.0249(2)	0.25	−0.0048(4)	A	0.0348(2)	0.25	−0.0061(4)	A	0.0400(2)	0.25	−0.0077(4)
Mn	0	0	0.5	Mn	0	0	0.5	Mn	0	0	0.5
O_1	0.4904(4)	0.25	0.0656(4)	O_1	0.4864(3)	0.25	0.0729(4)	O_1	0.4837(2)	0.25	0.0752(3)
O_2	0.2803(3)	0.0332(2)	−0.2784(3)	O_2	0.2882(2)	0.0378(2)	−0.2847(2)	O_2	0.2917(2)	0.0393(1)	−0.2875(2)
Mn–O distances				Mn–O distances				Mn–O distances			
$Mn–O_1$	1.9615(4) Å × 2			$Mn–O_1$	1.9596(4) Å × 2			$Mn–O_1$	1.9567(3) Å × 2		
$Mn–O_2$	1.968 (2) Å × 2			$Mn–O_2$	1.983 (1) Å × 2			$Mn–O_2$	1.992 (1) Å × 2		
$Mn–O_2$	1.955 (2) Å × 2			$Mn–O_2$	1.953 (1) Å × 2			$Mn–O_2$	1.953 (1) Å × 2		
Mn–O–Mn angles				Mn–O–Mn angles				Mn–O–Mn angles			
$Mn–O_1–Mn$	158.70°			$Mn–O_1–Mn$	156.28°			$Mn–O_1–Mn$	155.41°		
$Mn–O_2–Mn$	159.90°			$Mn–O_2–Mn$	156.29°			$Mn–O_2–Mn$	154.90°		
Reliability factors				Reliability factors				Reliability factors			
$R_p = 4.15\%$				$R_p = 4.35\%$				$R_p = 4.05\%$			
$R_{wp} = 5.33\%$				$R_{wp} = 5.56\%$				$R_{wp} = 5.13\%$			
$\chi^2 = 2.23$				$\chi^2 = 2.28$				$\chi^2 = 1.92$			

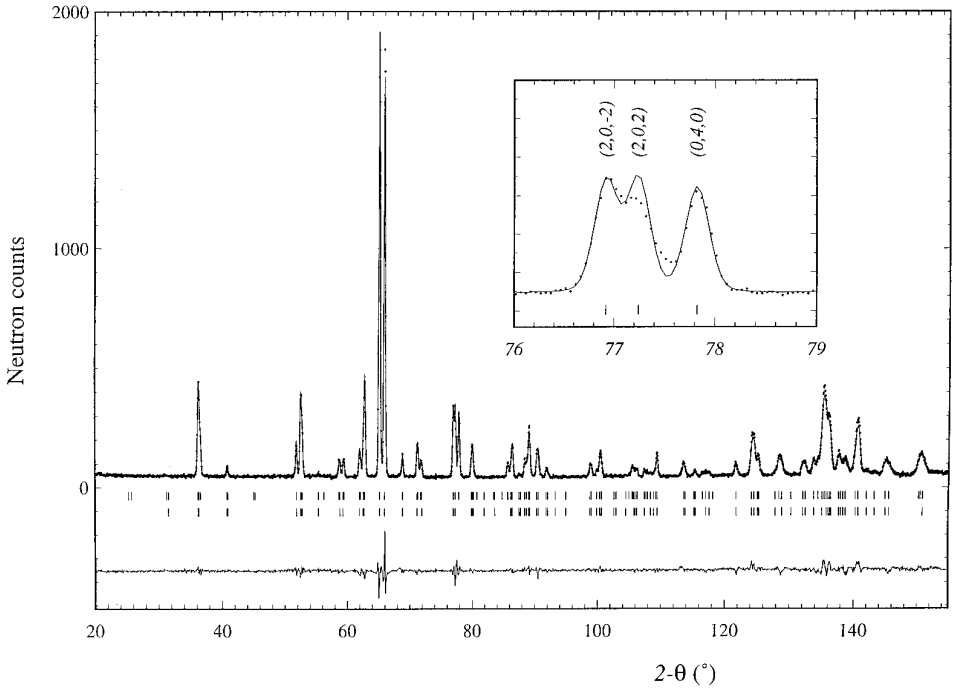

FIG. 2. Neutron powder diffraction refinement of $Nd_{0.7}Ca_{0.3}MnO_3$ at 1.7 K with a neutron wavelenght of 2.39 Å. In the profile, points are observed data, the solid line is the calculated pattern. The Bragg reflection tics are given for the nuclear structure (top) and magnetic structure (bottom). The inset shows the monoclinic splitting on the (202) Bragg peak.

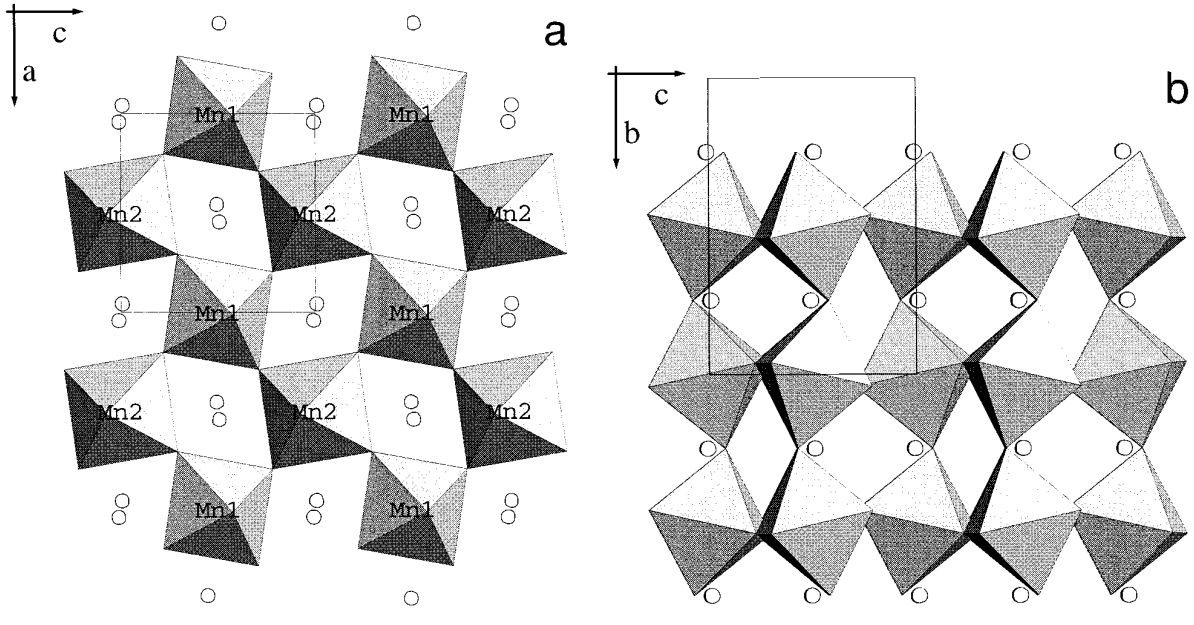

FIG. 3. (a) Projection of the $Nd_{0.7}Ca_{0.3}MnO_3$ structure along the *b* axis. (b) Projection of the $Nd_{0.7}Ca_{0.3}MnO_3$ structure along the *a* axis.

TABLE 2
Low-Temperature Structures

Space group: *Pnma*						Space group: $P2_1/m$			
$Nd_{0.7}Sr_{0.3}MnO_3$			$Nd_{0.7}Sr_{0.08}Ca_{0.22}MnO_3$			$Nd_{0.7}Ca_{0.3}MnO_3$			
Cell parameters			Cell parameters			Cell parameters			
a = 5.4494(1) Å			a = 5.4734(1) Å			a = 5.4881(1) Å			
b = 7.6964(1) Å			b = 7.6583(1) Å			b = 7.6337(1) Å		β = 90.20°	
c = 5.4547(1) Å			c = 5.4139(1) Å			c = 5.3968(1) Å			
Atomic coordinates			Atomic coordinates			Atomic coordinates			
	x	y	z	x	y	z	x	y	z
A	0.0259(2)	0.25	−0.0052(4)	0.0382(2)	0.25	−0.0070(4)	A_1 0.0421(5)	0.25	−0.0084(6)
Mn	0	0	0.5	0	0	0.5	A_2 0.5441(5)	0.25	0.5067(5)
O_1	0.4908(4)	0.25	0.0655(4)	0.4856(3)	0.25	0.0729(4)	Mn_1 0	0	0.5
O_2	0.2808(3)	0.0332(2)	−0.2785(3)	0.2909(2)	0.0377(2)	−0.2850(3)	Mn_2 0.5	0	0
							O_1 0.4837(6)	0.25	0.0756(6)
							O_2 0.9839(6)	0.25	0.4240(7)
							O_3 0.2918(4)	0.0412(5)	−0.2909(4)
							O_4 0.7967(4)	0.038(5)	0.7820(4)
Mn–O distances			Mn–O distances			Mn–O distances			
$Mn–O_1$	1.9576(4) Å × 2		$Mn–O_1$	1.9564(5) Å × 2		$Mn_1–O_2$	1.9539(8) Å × 2		
$Mn–O_2$	1.966 (1) Å × 2		$Mn–O_2$	1.993 (1) Å × 2		$Mn_1–O_3$	1.981 (1) Å × 2		
$Mn–O_2$	1.949 (1) Å × 2		$Mn–O_2$	1.943 (1) Å × 2		$Mn_1–O_4$	1.913 (1) Å × 2		
						$Mn_2–O_1$	1.9536(3) Å × 2		
						$Mn_2–O_3$	1.964 (1) Å × 2		
						Mn_2O_4	2.034 (1) Å × 2		
Mn–O–Mn angles			Mn–O–Mn angles			Mn–O–Mn angles			
$Mn–O_1–Mn$	158.76°		$Mn–O_1–Mn$	156.25°		$Mn_2–O_1–Mn_2$	155.30°		
$Mn–O_2–Mn$	159.81°		$Mn–O_2–Mn$	155.86°		$Mn_1–O_2–Mn_1$	155.24°		
						$Mn_1–O_3–Mn_2$	153.71°		
						$Mn_1–O_4–Mn_2$	155.19°		
Reliability factors			Reliability factors			Reliability factors			
R_p = 4.78%			R_p = 4.86%			R_p = 4.67%			
R_{wp} = 6.08%			R_{wp} = 6.13%			R_{wp} = 5.86%			
χ^2 = 1.99			χ^2 = 2.02			χ^2 = 1.80			

(40%). The Mn(2) site, however, has an average Mn–O distance of 1.98 Å; it can thus be supposed that it is occupied uniquely by Mn^{3+} ions, since the sum of the ionic radii of Mn^{3+} and O^{2-} in sixfold coordination is approximately 1.98 Å (13). This evidence for ordering of the Mn^{3+} and Mn^{4+} ions is strongly supported by the difference in the Jahn–Teller distortion of the MnO_6 octahedra (Table 2). With Mn–O distances ranging from 1.953 to 2.033 Å, the Mn(2) octahedra that are uniquely occupied by Mn^{3+} are significantly more distorted than the Mn(1) octahedra (1.913 to 1.981 Å) that are randomly occupied by Mn^{3+} and Mn^{4+} ions. Thus, as shown from the projections of the $[MnO_2]_\infty$ framework of this low-temperature phase along b (Fig. 3a) and along a (Fig. 3b), the structure is built up of two kinds of rows of MnO_6 octahedra. These rows labeled Mn(1) and Mn(2), running along b, are arranged in an ordered fashion, and are occupied by mixed "Mn^{3+}/Mn^{4+}" and Mn^{3+} ions, respectively. Note the [001] diamond-shaped tunnels formed by the MnO_6 octahedra (Fig. 3a) and the antiphase modulation of the $[MnO_2]_\infty$ layers that order parallel to (010) (Fig. 3b). Moreover the elongated O–Mn–O bonds alternate with shorter ones along the [110] and $[1\bar{1}0]$ directions.

In contrast to the room temperature powder patterns, those recorded at 1.7 K show a ferromagnetic contribution on some nuclear peaks, irrespective of x. At this low temperature, the ferromagnetic scattering arises from both manganese and neodymium, with magnetic moments oriented along the b axis. The magnitude of the magnetic moments does not vary significantly with x, ranging from 3 μ_B (x = 0) to 3.4 μ_B (x = 0.30) for manganese and from 1.2 μ_B (x = 0) to 0.8 μ_B (x = 0.30) for neodymium. This

ferromagnetic contribution to the neutron data at low temperature is in agreement with magnetization measurements that show a transition from a paramagnetic to a ferromagnetic state as T decreases, for all x ; T_c ranges from 210 K for $Nd_{0.7}Sr_{0.3}MnO_3$ ($x = 0.30$) to 130 K for $Nd_{0.7}Ca_{0.3}MnO_3$ ($x = 0$).

In conclusion, we have shown that in the manganite $Nd_{0.7}Ca_{0.3-x}Sr_xMnO_3$ series, a transition from orthorhombic to monoclinic symmetry occurs as the average size of the interpolated cations decreases. The most important feature of this study concerns the evidence for the appearance of a new kind of charge ordering in $Nd_{0.7}Ca_{0.3}MnO_3$. This result may have considerable implications in explaining the CMR properties of all other manganites studied to date, in particular for manganites that exhibit a CMR effect in an applied magnetic field greater than 5 T, in spite of their insulating properties.

ACKNOWLEDGMENT

One of us (G.M.) thanks the EEC for the provision of a HCM fellowship.

REFERENCES

1. R. M. Kusters, J. Singleton, D. A. Keon, R. M. Greedy, and W. Hayes, *Physica B* **155,** 362 (1989).
2. K. Chahara, T. Ohno, M. Kasai, and Y. Kozono, *Appl. Phys. Lett.* **63,** 1990 (1993).
3. R. Von Helmholt, J. Wecker, B. Holzapfel, L. Schultz, and K. Samwer, *Phys. Rev. Lett.* **71,** 2331 (1993).
4. B. Raveau, A. Maignan, and V. Caignaert, *J. Solid State Chem.* **117,** 424 (1995).
5. K. Knizek, Z. Jirak, E. Pollert, F. Zounova, and S. Vratislav, *J. Solid State Chem.* **100,** 292 (1992).
6. Y. Tomioka, A. Asumitsu, Y. Moritomo, H. Kuwahara, and Y. Tokura, *Phys. Rev. Lett.* **74,** 5108 (1995).
7. P. E. Schiffer, A. P. Ramirez, W. Bao, and S.-W. Cheong, *Phys. Rev. Lett.* **75,** 3336 (1995).
8. C. H. Chen and S.-W. Cheong, *Phys. Rev. Lett.* **76,** 4042 (1996).
9. A. Maignan, C. Simon, V. Caignaert, and B. Raveau, *J. Appl. Phys.* **79,** 7891 (1996).
10. H. Y. Hwang, S.-W. Cheong, P. G. Radaelli, M. Marezio, and B. Batlogg, *Phys. Rev. Lett.* **75,** 914 (1995).
11. F. Millange, A. Maignan, V. Caignaert, Ch. Simon, and B. Raveau, *Z. Phys. B,* in press.
12. V. Caignaert, E. Suard, A. Maignan, Ch. Simon, and B. Raveau, *J. Magn. Magn. Mater.* **L260,** 153 (1996).
13. R. D. Shannon, *Acta Crystallogr. Sect. A* **32,** 751 (1976).